HHS Public Access

Author manuscript

FASEB J. Author manuscript; available in PMC 2023 June 01.

Published in final edited form as:

FASEB J. 2022 June ; 36(6): e22364. doi:10.1096/fj.202101924R.

Dysregulation of the Scribble/YAP/β-catenin axis sustains the fibroinflammatory response in a PKHD1$^{-/-}$ mouse model of Congenital Hepatic Fibrosis

Luca Fabris[1,2,3], **Chiara Milani**[4], **Romina Fiorotto**[3], **Valeria Mariotti**[1,3,†], **Eleanna Kaffe**[3,‡], **Barbara Seller**[4,§], **Aurelio Sonzogni**[5], **Mario Strazzabosco**[3,*], **Massimiliano Cadamuro**[1,2,*]

[1]Department of Molecular Medicine (DMM), University of Padova, Padova, Italy;

[2]International Center for Digestive Health (ICDH), University of Milan-Bicocca, Milan, Italy;

[3]Liver Center, Department of Internal Medicine, Yale University, New Haven (CT), US;

[4]School of Medicine and Surgery, University of Milan-Bicocca, Milan, Italy;

[5]Department of Pathology, ASST Papa Giovanni XXIII Hospital, Bergamo, Italy.

Abstract

Congenital hepatic fibrosis (CHF), a genetic cholangiopathy characterized by fibropolycystic changes in the biliary tree, is caused by mutations in the *PKHD1* gene, leading to defective fibrocystin (FPC), changes in planar cell polarity (PCP) and increased β-catenin-dependent chemokine secretion. In this study, we aimed at understanding the role of Scribble (a protein involved in PCP), YAP and β-catenin in the regulation of the fibroinflammatory phenotype of FPC-defective cholangiocytes. Immunohistochemistry showed that compared with WT mice, in FPC-defective (*Pkhd1*$^{del4/del4}$) mice nuclear expression of YAP/TAZ in cystic cholangiocytes, significantly increased and correlated with CTGF expression and pericystic fibrosis, while Scribble expression on biliary cyst cells was markedly decreased. Cholangiocytes isolated from WT mice showed intense Scribble immunoreactivity at the membrane, but minimal nuclear expression of YAP, which conversely increased, together with CTGF, after siRNA silencing of Scribble. In FPC-defective cholangiocytes, inhibition of YAP nuclear import reduced β-catenin nuclear expression, and CTGF, integrin β6, CXCL1, and CXCL10 mRNA levels, whereas inhibition of β-catenin signalling did not affect nuclear translocation of YAP. Notably, siRNA silencing of Scribble and YAP in WT cholangiocytes mimics the fibroinflammatory changes of

[*]**Corresponding authors**: Mario Strazzabosco, MD, PhD, Department of Internal Medicine, Yale University School of Medicine, Cedar Street 333 Room LMP1080, New Haven, CT 06517, USA. Phone: +1-203-785-5110, mario.strazzabosco@yale.edu, Massimiliano Cadamuro, PhD, Department of Molecular Medicine, University of Padova, Gabelli Street 63, Padova, 35121, Italy. Phone: +39-049-827-6113, massimiliano.cadamuro@unipd.it.

[†]Neuroimmunology Unit, INSpe, Division of Neuroscience, San Raffaele Scientific Institute, Milan, Italy;

[‡]Department of Immunobiology, Yale University, New Haven (CT), US;

[§]Department of Gastroenterology, Hepatology and Endocrinology, Hannover Medical School, Hannover, Germany.

Author contributions: LF, MS, MC designed the experiments, wrote the manuscript and supervised the project. RF contributed in writing and in revising the manuscript. EK generated the double KO mice, RF performed breeding and experiments on mice. AS collected and analyzed human tissue samples. CM, RF, BS, analyzed mouse tissue samples. CM, VM, BS, MC performed and analyzed *in vitro* experiments.

Conflict of interest statement: MS is member of the advisory board of Engitix; LF has received honorarium from L.E.K. Consulting; other authors declared that have nothing to disclosure.

FPC-defective cholangiocytes. Conditional deletion of β-catenin in *Pkhd1*$^{del4/del4}$ mice reduced cyst growth, inflammation and fibrosis, without affecting YAP nuclear expression. In conclusion, the defective anchor of Scribble to the membrane facilitates the nuclear translocation of YAP and β-catenin with gain of a fibroinflammatory phenotype. The Scribble/YAP/β-catenin axis is a critical factor in the sequence of events linking the genetic defect to fibrocystic trait of cholangiocytes in CHF.

Keywords

chronic cholangiopathy; congenital hepatic fibrosis; Scribble; YAP; fibrocystin

INTRODUCTION

Fibropolycystic liver diseases are a group of developmental cholangiopathies that include congenital hepatic fibrosis (CHF) and Caroli disease (CD), two disorders with autosomal recessive inheritance and characterized by saccular cyst-like biliary structures, accompanied by a robust inflammatory infiltrate preeminently with peribiliary localization (1). CHF/CD are diagnosed more frequently in adolescents or young adults, and their progression leads to portal hypertension, and variceal bleeding, eventually needing a liver transplant. Some cases may eventually develop cholangiocarcinoma (2,3). To date no pharmacological therapy is available to effectively treat these rare conditions that remain an unresolved issue for pediatricians and hepatologists.

Fibropolycystic cholangiopathies are caused by mutations in the *polycystic kidney and hepatic disease1* (*PKHD1*) gene, located on chromosome 6p21.1-p12 (4). Its gene product, fibrocystin/polyductin (FPC), is a large membrane protein expressed on the primary cilium, basal bodies, and tight/adherent junctions of ductal epithelial cells, including cholangiocytes. The role of fibrocystin is not completely understood, but it appears to be crucial in cell differentiation of ductal epithelia, as its loss of function causes malformations of the ductal plates (5). As recently shown, FPC function is needed also in adult life (6).

The pathobiology of CHF is not well understood, however, recent studies in orthologous mouse models of CHF have shown that FPC-defective cholangiocytes present several signaling defects (7–9). Among these, an increased transcriptional activity of β-catenin leads to the secretion of chemokine (C-X-C motif) ligand (CXCL)1, CXCL10, and CXCL12, involved in the recruitment of inflammatory cells, along with integrin β6, the local activator of transforming growth factor (TGF)-β1 leading to peri-cystic fibrogenesis (10).

The hypothesis behind our study is that increased β-catenin signaling may be secondary to changes in YAP/TAZ signaling. Yes-associated protein (YAP) and its companion transcriptional coactivator with PDZ-binding motif (TAZ) are components of the β-catenin destruction complex (11). The YAP/TAZ complex is usually bound to the β-catenin destruction complex in a phosphorylated, inactive form (11). This complex is maintained docked at the cell-cell junctions by Scribble, a membrane protein that is involved in the maintenance of the planar cell polarity (PCP) of ductal epithelia (12,13). Once Scribble disaggregates from its anchor site, YAP can be dephosphorylated and translocated together

with TAZ to the nucleus. YAP and TAZ, when imported into the nucleus act as transcription factors mediating the signal transduction of Hippo pathway, an evolutionary conserved signal cascade supervising several physiological and pathological cellular responses (14). Upon entering the nucleus, YAP binds to its transcriptional enhanced associate domains (TEAD1–4) to unfold a transcriptional program. It has been proposed that YAP/TAZ, by detaching from the β-catenin destruction complex, block the degradation of β-catenin that then accumulates in the cytoplasm, translocate into the nucleus, and binds to the T-cell factor/lymphoid enhancer factor (TCF/LEF) family members to become transcriptionally active (14).

Starting from these observations, we aimed at investigating if a crosstalk between Scribble, YAP/TAZ and β-catenin, promotes the pro-inflammatory and pro-fibrotic epithelial phenotype typical of FPC-deficiency. We also tested if pharmacological or genetic manipulation of the Scribble/YAP/β-catenin axis results in a reduction of secreted mediators relevant for inflammatory cell recruitment and fibrosis deposition.

MATERIALS AND METHODS

Isolation, characterization, culture and treatment of cholangiocytes.

Mouse cholangiocytes were isolated from *Pkhd1*$^{del4/del4}$ and wild type (WT) mice at 3 months of age and cultured as previously described (10).

The culture medium was composed by Dulbecco's Modified Eagle Medium/Ham's F12 supplemented with fetal bovine serum (10%), MEM nonessential amino acids solution (1%), MEM vitamin solution (1%), insulin-transferrin-selenium-x (1%), chemically defined lipid concentrate (1%), soybean trypsin inhibitor (50μg/ml), l-glutamine (1%), penicillin/streptomycin (1%), gentamycin (0,5%), dexamethasone (393μg/ml, Sigma-Aldrich, St. Louis, MO, USA), triiodothyronine (3,4mg/ml, Sigma-Aldrich, St. Louis, MO, USA), EGF (25μg/ml, Sigma-Aldrich, St. Louis, MO, USA), and forskolin (10uM, Sigma-Aldrich, St. Louis, MO, USA), all supplied by ThermoFisher Scientific (Waltham, MA, USA), unless otherwise indicated. Cells were cultured in flasks or multiwells precoated with rat-tail collagen. *Pkhd1*$^{del4/del4}$ cholangiocytes were treated with inhibitors of YAP nuclear import Dobutamine (Dob, 20μM, 24h; Sigma-Aldrich, St. Louis, MO, USA) (15), Y27632 (Y, 10μM, 24h; Sigma-Aldrich, St. Louis, MO, USA) (16), Latrunculin A (Lat A, 1μM, 1h; Santa Cruz Biotechnology, Dallas, TX, USA) (17), and with Verteporfin (VP, 20μM, 24h; ForLab, Bruxelles, Belgium) (18), an inhibitor of YAP transcriptional activity. IGC-001 (25μM, 24h; Sigma-Aldrich, St. Louis, MO, USA) (10) was used to block β-catenin transcriptional activity.

Animal model.

We used the *Pkhd1*$^{del4/del4}$ mouse (a kind gift from S. Somlo, Yale University, New Haven, CT), an orthologue model of the human CHF (19). *Pkhd1*$^{del4/del4}$ mice were generated on a mixed C57BL6/129Sv background, harboring an inactivating deletion in the exon 4 of the *Pkhd1* gene (orthologous of the human *PKHD1*), while WT littermates of the same genetic background served as controls. To generate Pkhd1/β-catenin liver specific double KO mice

we crossed *Pkhd1*$^{del4/del4}$ mice with AlbCre mice (B6.FVB(129)-Tg(Alb1-cre)1Dlr/J) and β-catenin$^{fl/fl}$ (B6.129-*Ctnnb1*^{tm2Kem}/KnwJ) that were obtained from Jackson Laboratories (Bar Harbor, ME, USA). All mice were maintained at the Yale Animal Resources Center and used according to a protocol approved by the Yale University Institutional Animal Care and Use Committee (IACUC) and the Office of Animal Research Support (OARS) of Yale University. After mouse sacrifice, liver tissue was harvested, fixed in formalin, and embedded in paraffin.

Human tissues samples of CHF and control livers.

Formalin-fixed, paraffin-embedded de-identified archival tissue specimens of CHF patients obtained from liver transplant explants (n=2) or liver resection (n=1) were used for the immunohistochemical study. As controls (normal liver, NL), wedge biopsies from liver grafts implanted for liver transplant (n=5) were used. All specimens were reviewed by a pathologist (AS) to confirm the diagnosis of CHF.

Immunohistochemistry.

The expression of YAP (Cell Signaling, Danvers, MA, USA), TAZ (Sigma-Aldrich, St. Louis, MO, USA), K19 (Hybridoma Bank University of Iowa, USA), Scribble, connective tissue growth factor (CTGF) (both Santa Cruz Biotechnology, Dallas, TX, USA), β-catenin and CD45 (both BD Pharmingen, San Diego, CA, USA) were assessed by immunohistochemistry in formalin-fixed paraffin-embedded specimens. Briefly, after deparaffinization using xylene, sections were rehydrated in absolute ethanol (all from Carlo Erba, Cornaredo, Italy) and then washed in tap water; endogenous peroxidase activity was quenched incubating slides with methanol containing 10% H_2O_2 (Carlo Erba, Cornaredo, Italy) for 15mins. Following the proper antigen retrieval (see Supplementary Table 1), unspecific binding was blocked using UltraVision protein block (ThermoFisher Scientific, Waltham, MA, USA) for 8mins. The sections were then incubated overnight at 4°C with primary antibodies diluted in phosphate-buffered saline (PBS) + BSA 1% (Sigma-Aldrich, St. Louis, MO, USA) (see Supplementary Table 1). After rinsing with PBS 1M supplemented with 0.05% Tween20 (PBS-T; both Sigma-Aldrich, St. Louis, MO, USA), slides were incubated for 30mins at room temperature with the specific horseradish peroxidase (HRP)-conjugated secondary antibody (EnVision, Agilent Technologies, Santa Clara, CA, USA). Specimens were developed using 3,3-diaminobenzedine tetrahydrochloride (DAB, Abcam, Cambridge, UK), counterstained with Gill's Hematoxylin N°2 (Sigma-Aldrich, St. Louis, MO, USA), and mounted using EuKitt (Bio-Optica, Milan, Italy).

Histochemical staining for Sirius Red.

Following deparaffinization and hydration, as above described, sections were placed for 2mins in 0.2% phosphomolybdic acid, rinsed in tap water and then incubated for 60mins in 0.1% Sirius red (Direct Red 80) in saturated picric acid pH 2.0 (all from Sigma-Aldrich, St. Louis, MO, USA). Sections were then rinsed in 0.5% glacial acetic acid (Carlo Erba, Cornaredo, Italy) and then dehydrated and mounted using EuKitt (Bio-Optica, Milan, Italy).

Analysis of nYAP, nTAZ, Sirius Red, and CTGF expression.

Following immunostaining, nuclear expression of YAP (nYAP), and TAZ (nTAZ) was assessed in four samples of *Pkhd1*$^{del4/del4}$ mice for each age (1, 3, 6, 9 and 12 months) and in 6-month-old WT mice. Five randomly taken micrographs at 10x were collected from each sample using Eclipse E800 microscope equipped with a cooled DS-U1 digital camera and then analyzed using LuciaG 5.0 software (all from Nikon Instruments, Campi Bisenzio, Italy). The nuclei positive for YAP and TAZ in biliary structures (ducts and cysts) were counted and expressed as percentage of positive nuclei over the total count of nuclei of the biliary structures. Extent of CTGF, K19, CD45 and Sirius Red were evaluated by ImageJ in five-ten randomly taken micrographs at 10x or a whole lobule at 4x for K19, and calculated as percentage of pixels above the threshold value with respect to the total pixels per field, and normalized on cyst area.

Western blotting (WB) for total cell lysate and for nuclear/cytoplasmic fraction.

By WB, we assessed the expression of YAP (Cell Signaling, Danvers, MA, USA), TAZ (Sigma-Aldrich, St. Louis, MO, USA), CTGF (Santa Cruz Biotechnology, Dallas, TX, USA), β-catenin (BD Pharmingen, San Diego, CA, USA) and Scribble (Bio-Techne, Abingdon, UK) in total lysate or cellular fractions (nucleus/cytoplasm) of *Pkhd1*$^{del4/del4}$ and WT cholangiocytes. Nuclear/cytoplasmic fractions were obtained using the Ne-Per kit (ThermoFisher Scientific, Waltham, MA, USA) following the manufacturer protocol, whilst total cell lysate using Cell-Lytic (Sigma-Aldrich, St. Louis, MO, USA). Equal amounts of proteins were mixed with 4–12% NuPAGE Sodium Dodecyl Sulphate (SDS) sample buffer and electrophoresed on a 4–12% SDS-PAGE precast gel. Proteins were transferred to nitrocellulose 0.4μm pore-size membrane (all from ThermoFisher Scientific, Waltham, MA, USA). Membranes were incubated with 5% dry milk in Tris-buffered saline (TBS) containing 0.1% Tween 20 (Euroclone, Pero, Italy) (TBST) for 1h at room temperature to block all the non-specific sites. After blocking, blots were incubated overnight at 4°C with the specific primary antibodies, all diluted in TBST + milk 5% (see Supplementary Table 1). Actin, histone 3H (Sigma-Aldrich, St. Louis, MO, USA), or Na/K ATPase (Abcam, Cambridge, UK) were used as normalizing proteins. Nitrocellulose membranes were washed with PBST and then incubated for 1h at room temperature with anti-rabbit and anti-mouse secondary antibodies (1:2000, Sigma-Aldrich, St. Louis, MO, USA), diluted in TBST + milk 5%. Enhanced chemiluminescence was used to visualize proteins (ECL West Pico or Dura, Euroclone, Pero, Italy). The intensity of the band was quantified using ImageJ program.

Immunofluorescence and relative fluorescence analysis (RFA).

Cells were plated on 20mm coverslips coated with rat-tail collagen: *Pkhd1*$^{del4/del4}$ or WT mouse cholangiocytes were seeded at 20.000 cells/insert. After adhesion, *Pkhd1*$^{del4/del4}$ cholangiocytes were treated with the YAP inhibitors, Dob, Y, Lat A, and VP, or with siRNAs against Scribble. After fixation with paraformaldehyde 4% (PFA) for 15mins at room temperature, cells were washed with PBS 1x. Cells were permeabilized for 10mins in PBS/TritonX-100 0.1%, unspecific binding sites were blocked with UltraVision Protein Block (ThermoFisher Scientific, Waltham, MA, USA,) for 10mins at room temperature (RT) and then incubated overnight at 4°C with the primary antibodies for YAP, TAZ, K19 (specific

biliary marker), ZO-1 (marker of tight junctions) (ThermoFisher Scientific, Waltham, MA, USA), and Scribble (Santa Cruz Biotechnology, Dallas, TX, USA) (see Supplementary Table 1). Cells were then incubated with the proper secondary antibody for 45mins at room temperature (Alexa Flour 594 or Alexa Fluor 488 (1:500; ThermoFisher Scientific, Waltham, MA, USA), and mounted using Vectashield supplemented with 4',6-diamidino-2-phenylindole (DAPI) (Vector Laboratories, Burlingame, CA, USA). RFA analysis was performed by taking random pictures at 200x for each well using an Eclipse E800 microscope. For each picture, the intensity of nuclear YAP and TAZ was evaluated in 10 nuclei: the fluorescence channels were separated and the peak of red signal (YAP/TAZ) in the nucleus (blue signal) was analyzed twice by LuciaG 5.0 software (20,21).

Silencing of Scribble.

Gene silencing of Scribble was performed using commercially available specific siRNAs and scramble RNA served as control (both Santa Cruz Biotechnology, Dallas, TX, USA Biotechnology). After plating, WT mouse cells were transfected using 33nM of siRNA and Lipofectamine 2000 transfection reagent (ThermoFisher Scientific, Waltham, MA, USA) and analyzed after 48 hours. Successful silencing of Scribble was confirmed by WB and immunofluorescence.

Gene expression assessment by Real-Time PCR (RT-PCR).

Total RNA was isolated from *Pkhd1*$^{del4/del4}$ cholangiocytes treated with the above-described YAP inhibitors and compared with WT cholangiocytes as controls, using Trizol reagent and quantified by Nanodrop 1000' spectrometer. One-μg RNA was converted into cDNA using a high capacity cDNA reverse transcription kit; 50ng of cDNA was used to perform real time PCR experiments using TaqMan probes for CTGF, CXCL1, CXCL10, and β6 integrin subunit. Data were normalized using GAPDH as housekeeping gene and analyzed using the ΔCt method. All reagents were supplied by ThermoFisher Scientific, Waltham, MA, USA.

Statistical analysis.

Results were shown as mean ± standard deviation (SD). Statistical comparisons were made using Student's t-test or one-way ANOVA analysis with Tukey's multiple comparison test, where appropriate. Correlation analysis were performed using the Pearson's correlation coefficient. Statistical analyses were performed using PRISM 9 (GraphPad Software, La Jolla, CA, USA). A 2-tailed p value <0.05 was considered significant.

RESULTS

In *Pkhd1*$^{del4/del4}$ mice, nuclear expression of YAP and TAZ in biliary structures increases over time, whilst that of Scribble is down-regulated.

Consistent with a prior report by Jiang and coll. in the PCK rat model of CHF (22), immunohistochemistry showed that nuclear expression of nYAP and nTAZ were increased in the biliary cysts and microhamartomas of *Pkhd1*$^{del4/del4}$ mice. By comparing liver sections from *Pkhd1*$^{del4/del4}$ mice at different ages with liver samples from a 6-month-old WT mouse, we observed that both nYAP and nTAZ (Figure 1A,B) increased in a time-dependent fashion in mutated mice. This increase was significant since the earliest age (1

month) with respect to WT, where both nYAP and nTAZ resulted nearly negative. On the other hand, the membrane expression of Scribble was positive in WT mice but was absent in biliary cysts and microhamartomas since the earliest maturation age (Figure 1A). These findings were reproduced in human archival biopsies of CHF and NL where membrane expression of Scribble resulted uneven or absent in biliary lesions of CHF, in contrast with normal bile ducts (Supplementary Figure 1). Moreover, biliary expression of both nYAP and nTAZ was strongly increased in samples of fibropolycystic disease, whilst it was substantially absent in controls (Supplementary Figure 1). These results indicate that the Scribble/YAP axis is perturbed in CHF.

In *Pkhd1*$^{del4/del4}$ mice, nYAP expression correlates with CTGF expression and fibrosis deposition.

CTGF is a matricellular protein endowed with strong fibrogenic functions due to its ability to interact with extracellular matrix components (fibronectin), cell surface glycoprotein receptors (integrins), and growth factors (TGFβ1). CTGF expression is a known downstream effector of YAP signaling (23–26) and therefore is considered a readout of YAP activation. In the *Pkhd1*$^{del4/del4}$ mouse, we observed a significant increase in the expression of CTGF, which correlated with the extent of fibrosis as measured by Sirius red, whereas it was negative in WT livers (Figure 2A–C). Of note, expression of both nYAP and nTAZ correlated with that of CTGF, and with the extension of the liver fibrosis evaluated by Sirius Red (Figure 2C). These data suggest that YAP signaling is functionally relevant in the fibrotic progression of the disease, and that CTGF can be one of the mediators of this effect.

Expression of nYAP is up-regulated in cultured *Pkhd1*$^{del4/del4}$ cholangiocytes and its nuclear translocation was inhibited by dobutamine, latrunculin A, and Y27632.

To further investigate the significance of YAP and TAZ nuclearization, we studied their nuclear-cytoplasmic shuttling by RFA (Figure 3A) in cholangiocytes isolated from *Pkhd1*$^{del4/del4}$ and WT mice (20,21). We found that expression of both nYAP and nTAZ was up-regulated in *Pkhd1*$^{del4/del4}$ cholangiocytes, compared with WT (Figure 3B–E, and Supplementary Figure 2 and 3). Up-regulation of nYAP and nTAZ in *Pkhd1*$^{del4/del4}$ cholangiocytes were also confirmed by WB analysis in isolated nuclear fractions (Figure 4B,C). Then, to dissect the mechanisms directing YAP and TAZ into the nucleus we used inhibitors able to interfere with their functions at different levels. Dobutamine (Dob), a synthetic agonist of β1-adrenergic receptors (27), inhibits YAP nuclear translocation through phosphorylation at the Ser127 residue, promoting its cytoplasmic retention (15). Y-27632 (Y), targeting Rho kinases, inhibits YAP nuclear access (28). Latrunculin A (Lat A) inhibits YAP nuclear entry, affecting F-actin polymerization and inducing cytoskeleton distress (17). VP acts instead as a pure inhibitor of YAP transcriptional activity by preventing YAP-TEAD binding, without affecting cytoskeleton dynamics (29,30). Consistent with the above, nYAP expression was significantly reduced by Dob, Y, and Lat A, but not by VP in *Pkhd1*$^{del4/del4}$ cholangiocytes (Figure 3B–E, and Supplementary Figure 2 and 3). In keeping with the *in-vivo* data, these *in-vitro* findings suggest that increased nuclear import of YAP is a key feature of FPC-mutated cholangiocytes and is regulated by a cytoskeleton-dependent mechanism (lack of effect with VP).

YAP modulated nuclear expression of β-catenin in *Pkhd1*$^{del4/del4}$ cholangiocytes.

Previous evidence indicate that nuclear translocation of YAP is an essential step of β-catenin migration into the nucleus, and a pre-requisite for its transcriptional activation (29). To test if this mechanism fits our model, we analyzed the effects of inhibitors of YAP nuclear import (Dob, Lat A, and Y) on β-catenin expression in *Pkhd1*$^{del4/del4}$ cholangiocytes. Consistent with the proposed working model, treatment with Dob and Y markedly reduced the nuclear expression of β-catenin (Figure 4A). Lat A treatment did not block β-catenin nuclear accumulation suggesting, that the actin cytoskeleton plays a differential role in the nuclear localization of the protein (31,32). On the other hand, β-catenin inhibition by ICG-001 had no effect on the nuclear localization of both YAP and TAZ (Figure 4B,C), consistent with YAP/TAZ driving β-catenin nuclearization, and not *vice versa*.

Scribble expression is reduced in *Pkhd1*$^{del4/del4}$ cholangiocytes also *in-vitro*.

Recent evidence showed that Scribble, a protein involved in PCP could modulate the Hippo pathway, and its absence, in Zebrafish, induced the formation of cyst-like lesion in the kidney (33). In contrast with WT cholangiocytes that, when double stained for Scribble and the tight junction marker ZO-1 showed a clear co-localization of the two proteins (Figure 5A), cholangiocytes isolated from *Pkhd1*$^{del4/del4}$ mice showed a much weaker membrane expression of Scribble in the context of a dysmorphic cell morphology (Figure 5A). Similarly, WB analysis of Scribble from cultured cells confirmed a reduced expression of the protein on membrane fractions (Figure 5B). In addition, real time PCR data, showed a significant downregulation of Scribble gene expression in *Pkhd1*$^{del4/del4}$ cholangiocytes (Supplementary Figure 4A).

To address the role of Scribble in YAP and TAZ nuclearization, we performed gene silencing in WT cells. The efficacy of Scribble inhibition by specific siRNAs was confirmed by IF and WB analysis of Scribble expression (Figure 5C, Supplementary Figure 4B and Supplementary Figure 5). Gene silencing of Scribble resulted in a concomitant significant increase in the nuclearization of YAP and TAZ (Figure 5C), consistent with the hypothesis that YAP/TAZ nuclearization is modulated by the presence of Scribble at the membrane. Interestingly, Scribble silencing resulted in a disarrangement of phalloidin-decorated actin microfilaments, further explaining the acquisition of a dysmorphic cell shape (Figure 5C, and Supplementary Figure 5) and consistent with the recognized role of Scribble in maintaining cell polarity. Notably, YAP nuclear shuttling induced by silencing of Scribble in WT cells was associated with its transcriptional activity, as shown by the up-regulated expression of CTGF (Figure 5D). Furthermore, silencing of Scribble induces a significant increase in nuclearization of β-catenin, consistent with our model (Figure 5E).

Manipulation of nYAP and Scribble modulates the fibroinflammatory phenotype of *Pkhd1*$^{del4/del4}$ and WT cholangiocytes.

To confirm the relevance of the Scribble/YAP/β-catenin axis in determining the fibroinflammatory phenotype of *Pkhd1*$^{del4/del4}$ cholangiocytes, we first tested the effects of YAP inhibitors on gene expression of a range of pro-infiammatory/fibrogenic mediators. In addition to CTGF, we evaluated CXCL1 and CXCL10, two chemokines previously shown to stimulate peribiliary macrophage infiltration, and αVβ6 integrin, the local activator of

latent TGFβ, previously shown to be up-regulated in cystic cholangiocytes in the same model and under the control of β-catenin (10). As shown in Figure 6A, upon treatment with YAP inhibitors (Dob, Lat A, Y, and VP), gene expression of CTGF, CXCL1, CXCL10 and β6 integrin, were significantly reduced in *Pkhd1*$^{del4/del4}$ cholangiocytes. Consistent with the above, a significant up-regulation of CTGF, CXCL10 and β6 integrin was observed in WT cells silenced for Scribble, (Figure 6B), further supporting the key role of Scribble in shaping the fibroinflammatory phenotype of cholangiocytes.

β-catenin deletion reduces the extent of disease in *Pkhd1*$^{del4/del4}$ mice.

Previous studies in *Pkhd1*$^{del4/del4}$ mice (10) and *in-vitro* results show that the transcriptional activity of β-catenin is the nodal point that mediates the fibroinflammatory response in CHF. The dysregulation of Scribble and the consequent nuclearization of YAP are prodromal to the transcriptional action of β-catenin and the secretion of chemokines able to recruit inflammatory cells around the cysts. To obtain further evidence of the role of β-catenin in the development and progression of CHF, we created *Pkhd1*$^{del4/del4}$/Alb-Cre^{+}Ctnnb1$^{flox/flox}$ double KO mice, i.e. *Pkhd1*$^{del4/de4}$ mice with specific deletion of β-catenin in the liver under the control of the albumin promoter. The efficiency of β-catenin deletion in cholangiocytes was confirmed by immunostaining, which showed β-catenin negativity in all cystic biliary structures and hepatocytes (Figure 7A). Notably, the larger bile ducts in the perihilar area, as well as the gallbladder epithelium still expressed β-catenin, as they do not activate the albumin-Cre promoter in keeping with their embryonic origin from the caudal part of the hepatic diverticulum (Supplementary Figure 6) (34). Hence, liver tissue in proximity of the peri-hilar area was excluded from the morphometric analysis. Consistent with our hypothesis, genetic deletion of β-catenin resulted in a significant reduction in the cystic area (40%) and in the extent of fibrosis (35%) in *Pkhd1*$^{del4/del4}$/Alb-Cre^{+}Ctnnb $^{flox/flox}$ mice with respect to *Pkhd1*$^{del4/de4}$ mice (Figure 7B,C). Peribiliary inflammatory cells were also reduced, as β-catenin deletion caused a 40% reduction in the inflammatory infiltrate (measured as CD45^{+} area) in *Pkhd1*$^{del4/del4}$/Alb-Cre^{+}Ctnnb1$^{flox/flox}$ mice with respect to *Pkhd1*$^{del4/del4}$ mice (Figure 7D). We cannot exclude that the changes in fibrosis and inflammatory infiltrate may be secondary to a reduced cystic burden, however, these results confirm the fundamental role of activated β-catenin signaling in the progression of the disease in CHF. Of note, nuclear expression of nYAP in *Pkhd1*$^{del4/del4}$/Alb-Cre^{+}Ctnnb1$^{flox/flox}$ was not affected, consistent with the hypothesis that YAP is instrumental for β-catenin nuclear import, but not *vice versa* (Figure 7A).

DISCUSSION

CHF represents a unique disease model in which genetically determined perturbations of cholangiocyte intracellular signaling are responsible for a proinflammatory/profibrotic epithelial phenotype, architectural changes, chronic inflammation and marked fibrogenesis (3,10). In this study, we show that FPC deficiency is associated with mis-localization and down-regulation of Scribble, increased nuclear import of both YAP and TAZ, and activation of β-catenin signaling, that results in increased expression of CTGF, CXCL1, CXCL10, and β6 integrin, the fundamental mediators of peribiliary inflammation and fibrosis in CHF (10).

Prior studies in the PKC rat model identified defects in cAMP and in Ca^{2+} signaling and in the PKA/RAF/ERK1/2 pathways (35). These observations explain the increased proliferation of cystic cholangiocytes, but do not easily account for the extensive peribiliary fibrotic response typical of fibropolycystic diseases. Our previous observations generated in an orthologous mouse model characterized by a deletion of exon 4 in the *Pkhd1* gene (*Pkhd1*$^{del4/del4}$ mouse) (19), showed that increased β-catenin signaling and production of pro-inflammatory mediators (i.e. CXCL1 and CXCL10), along with integrin αvβ6 up-regulation, are part of a repertoire of changes observed in FCP-defective cholangiocytes, resulting in increased recruitment of macrophages and fibroblasts (10). Studies from Jinag et al., (22) reporting an increased nuclear expression of YAP in biliary lesions of PKC rats, lead us to hypothesize a relationship between increased nuclear translocation of YAP/TAZ and the increased β-catenin signaling.

Recent studies suggested a cross talk between β-catenin and YAP/TAZ signaling (11,29). YAP and TAZ, the main effectors of the Hippo pathway, participate to the destruction complex that is responsible for the cytoplasmic degradation of β-catenin (11,29). Detachment of YAP from the destruction machinery and its transport into the nucleus prevents β-catenin inactivation, allowing β-catenin to translocate into the nucleus and to become transcriptionally active after interacting with TCF/LEF. A similar cooperation between YAP/TAZ and β-catenin has been shown to drive cell proliferation and invasion in breast cancer (36).

We therefore assessed the expression of YAP/TAZ in biliary lesions of both mouse and human liver samples and correlated the nuclear expression of YAP/TAZ with the expression of CTGF and with the deposition of pericystic fibrosis. In the *Pkhd1*$^{del4/del4}$ mouse, nuclear expression of YAP (nYAP) and TAZ (nTAZ) in biliary structures progressively increased in a time-dependent fashion, beginning with the earliest stages. Notably, in sections of human normal livers, expression of nYAP and nTAZ in biliary structures was weak, while it became intense and diffuse in the biliary cysts embedded in the large fibrotic areas in sections of CHF livers (Figure 1A and supplementary figure 1).

As readout of YAP/TAZ activation, we studied the expression of CTGF, a matricellular protein that plays several functions relevant to fibrogenesis and is increased in fibrotic livers (37). On the contrary to WT, *Pkhd1*$^{del4/del4}$ mice showed a time-dependent increase in the expression of CTGF that significantly correlated with the extent of fibrosis. Indeed, nYAP and nTAZ expression directly correlated with both CTGF expression and fibrosis.

Earlier studies in ARPKD (the kidney phenotype of fibropolycystic cholangiopathies) provided evidence for an altered planar cell polarity (PCP) signaling in ductal epithelia (38,39). PCP confers to cells the ability to align in the plane of the tissue, a property essential in ductal morphogenesis. This process involves the cooperation of different pathways including non-canonical WNT/β-catenin and multiple proteins expressed at the cellular junctions (39). Among these, Scribble, a tight junction-associated protein responsible for maintaining the planar configuration of ductal epithelia, has been shown to modulate the activation of the Hippo pathway in Zebrafish (33,40). Scribble is bound to the cell membrane where it maintains the YAP/TAZ complex in a phosphorylated and inactive

state. When Scribble detaches from the cell membrane, it allows YAP to dephosphorylate and to become activated (33). Therefore, we assessed the expression of Scribble together with that of YAP/TAZ in biliary lesions of both mouse and human liver samples. In WT livers, Scribble was expressed by normal bile ducts with a membranous pattern that was instead negligible in *Pkhd1*$^{del4/del4}$ mice and accompanied by increased nuclear expression of YAP (nYAP) and TAZ (nTAZ) on cystic structures. A similar pattern of expression was confirmed in NL and CHF livers.

To understand the mechanistic connection between Scribble, YAP/TAZ and β-catenin, and their relationship with the pro-inflammatory secretory phenotype of FPC-defective cholangiocytes, we studied cultured cholangiocytes obtained from 3-month old *Pkhd1*$^{del4/del4}$ mice and compared them with cholangiocytes isolated from WT mice of the same age. We confirmed the constitutive aberrant expression of both transcription factors in the nucleus of *Pkhd1*$^{del4/del4}$ cholangiocytes by either WB analysis in cell fractions or immunofluorescence. As expected, YAP and TAZ nuclear expression was inhibited by Dob, Lat A, and Y, but not by VP, which unlike the other compounds, inhibits YAP/TAZ transcriptional activity by preventing the connection with TEADs but not their nuclear shuttling.

We next evaluated the nuclear expression of β-catenin before and after inhibition of YAP nuclear translocation and transcriptional activation in *Pkhd1*$^{del4/del4}$ cholangiocytes. In contrast with VP (transcriptional inhibitor), Dob and Y treatments blunted β-catenin nuclear expression in cultured *Pkhd1*$^{del4/del4}$ cholangiocytes, thus indicating that the modulatory effect of YAP on β-catenin relies on its nuclear translocation and not on its interaction with TEAD. On the other hand, inhibition of β-catenin by ICG-001 (41), did not affect nuclear expression of both YAP and TAZ. These data are in line with a previous study (11,42), but at variance with other observations reporting a positive loop in which YAP nuclearization stimulates β-catenin activation that, in turn, further enhances YAP nuclearization (43). This discrepancy may indicate that there is a close interplay between YAP and β-catenin, but the directionality is tissue and cell-dependent. In fact, consistent with our *in-vitro* data, in mice double KO for PKHD1 and β-catenin (*Pkhd1*$^{del4/del4}$/Alb-Cre^{+}Ctnnb1$^{flox/flox}$), nuclear expression of nYAP was preserved.

The functional relevance of the relationship of YAP with β-catenin in FPC-defective cholangiocytes was analyzed by assessing the expression of CTGF and integrin βv6, together with that of the pro-inflammatory chemokines CXCL1 and CXCL10 (10), upon treatment with the abovementioned inhibitors. Consistent with our hypothesis, *Pkhd1*$^{del4/del4}$ cholangiocytes showed a significant decrease in CTGF expression once challenged with all YAP inhibitors. A similar reduction was obtained for integrin β6 that was more pronounced with Lat A, Y and VP, with levels comparable to WT cells.

By comparing cholangiocytes isolated from *Pkhd1*$^{del4/del4}$ and WT mice, we confirmed that the membranous expression of Scribble was strongly reduced in *Pkhd1*$^{del4/del4}$ cells, as it was its gene expression. Furthermore, silencing Scribble in WT cholangiocytes induced a significant increase in nYAP and nTAZ levels, and of β-catenin, in association with up-regulation of CTGF expression, consistent with a direct relationship of Scribble with

nYAP/nTAZ. Silencing Scribble in WT cholangiocytes also increased gene expression of integrin β6 and CXCL10.

The relationships between Scribble and FPC remain to be elucidated, but hypothetically, they may depend on their direct physical interaction or alternatively, on the presence of shared signaling pathways. Currently, little is known regarding the regulators of Scribble. CHF cholangiocytes, as demonstrated in PCK rat, are characterized by low intracellular concentrations of Ca^{2+} and augmented cAMP, resulting in increased proliferation (44,45). Deregulation of intracellular Ca^{2+} fluxes, could be one of the mechanisms that regulate FPC-Scribble interactions, but to date there are no data on this. Scribble can also be influenced by the presence of two complexes (Crumbs and Par) (46). However, the mechanisms that link the interaction between these factors are still far to be fully understood. While these speculations are worthy to be explored, our results are consistent with the following working model (Figure 8), in which, we hypothesize that a functional interaction between PKHD1 and Scribble. In cholangiocytes, Scribble, localized at the adherent junctions, retains YAP/TAZ into the cytoplasm in an inactive state. When fibrocystin is defective, Scribble detaches from the proper membranous site, thereby allowing YAP/TAZ to dephosphorylate, leave the β-catenin destruction complex and enter the nucleus (33). Once nuclearized, β-catenin together with YAP/TAZ, activates transcriptional programs generating a range of fibrogenic and inflammatory mediators (CTGF, integrin αVβ6, CXCL1 and CXCL10). Whereas a cooperation between YAP and β-catenin to stimulate cell proliferation in tumors has been well documented (47,48), their joint efforts in instructing cholangiocytes to gain pro-inflammatory and pro-fibrogenic functions represents a novel observation of potential translational consequences. Indeed, genetic deletion of β-catenin in cholangiocytes of *Pkhd1*$^{del4/del4}$ mice showed a significant decrease in cyst growth, inflammation and fibrosis. The decrease in the extent of these biliary lesions is the absence of β-catenin, as nYAP was preserved. Inhibition of β-catenin signaling is responsible for a lower local concentration of β-catenin-dependent profibrotic chemokines around the biliary structures resulting in a reduction of the pericystic inflammatory infiltrate. In turn, the reduced number of inflammatory cells account for a diminished secretion of cytokines trophic for the biliary epithelium, with a consequent reduction in the size of the cysts paralleled by a reduced deposition of fibrosis (49,50).

As fibropolycystic conditions represent a risk factor for cholangiocarcinoma, further studies should address if these mechanisms may have an oncogenic potential in cholangiocytes with FPC deficiency (3,51). If so, the Scribble/YAP-TAZ/β-catenin pathway may become promising target not only for fibropolycystic conditions, but also for biliary tract cancers (52).

Supplementary Material

Refer to Web version on PubMed Central for supplementary material.

Acknowledgements:

LF was supported by Progetti di Ricerca di Dipartimento (PRID) 2017, University of Padua, Italy; CM and MC were supported by Project Cariplo 2014 (cod: 2014-1099), Cariplo Foundation, Italy; RF and MS were supported

by NIH (R01 DK096096, and R01 DK101528). This project was supported in part by the Yale Liver Center award NIH P30 DK034989 Morphology and Cellular Molecular cores. The authors sincerely thank Prof. Paolo Simioni [General Internal Medicine and Thrombotic and Hemorrhagic Diseases Unit, Department of Medicine (DIMED), University of Padova, Italy] for the insightful suggestions and the critical revision of the manuscript.

Data availability statement:

The data that support the findings of this study are available from the corresponding author upon reasonable request.

Nonstandard abbreviations:

CHF	congenital hepatic fibrosis
CD	Caroli disease
PKHD1	*polycystic kidney and hepatic disease 1*
FPC	fibrocystin/polyductin
CXCL	chemokine (C-X-C motif) ligand
TGF-β1	transforming growth factor β1
YAP	Yes-associated protein
nYAP	nuclear Yes-associated protein
TAZ	transcriptional coactivator with PDZ-binding motif
nTAZ	nuclear transcriptional coactivator with PDZ-binding motif
PCP	planar cell polarity
TEADs	transcriptional enhanced associate domains
TCF/LEF	T-cell factor/lymphoid enhancer-binding factor
SCRIB	Scribble
WT	wild type
Dob	Dobutamine
Y	Y27632
Lat A	Latrunculin A
VP	Verteporfin
OARS	Office of Animal Research Support
CTGF	Connective tissue growth factor
K19	keratin 19

DAB	3,3-diaminobenzedine tetrahydrochloride, PFA, paraformaldehyde
PBS	Phosphate-buffered saline
BSA	bovine serum albumin
HRP	horseradish peroxidase
SDS	Sodium Dodecyl Sulphate
TBS	Tris-buffered saline
RFA	relative fluorescence analysis
ZO-1	zonula occludens-1
DAPI	4’,6-diamidino-2-phenylindole
siRNA	small interfering RNA
ANOVA	Analysis of Variance
ARPKD	autosomal recessive polycystic kidney disease

REFERENCES

1. Gunay-Aygun M. Liver and kidney disease in ciliopathies. Am J Med Genet C Semin Med Genet. 2009;151C(4):296–306. doi:10.1002/ajmg.c.30225 [PubMed: 19876928]
2. Khan SA, Toledano MB, Taylor-Robinson SD. Epidemiology, risk factors, and pathogenesis of cholangiocarcinoma. HPB (Oxford). 2008;10(2):77–82. doi:10.1080/13651820801992641 [PubMed: 18773060]
3. Fabris L, Fiorotto R, Spirli C, et al. Pathobiology of inherited biliary diseases: a roadmap to understand acquired liver diseases. Nat Rev Gastroenterol Hepatol. 2019;16(8):497–511. doi:10.1038/s41575-019-0156-4 [PubMed: 31165788]
4. Harris PC, Torres VE. Polycystic kidney disease. Annu Rev Med. 2009;60:321–337. doi:10.1146/annurev.med.60.101707.125712 [PubMed: 18947299]
5. Veigel MC, Prescott-Focht J, Rodriguez MG, et al. Fibropolycystic liver disease in children. Pediatr Radiol. 2009;39(4):317–421. doi:10.1007/s00247-008-1070-z [PubMed: 19083218]
6. Besse W, Roosendaal C, Tuccillo L, Roy SG, Gallagher AR, Somlo S. Adult Inactivation of the Recessive Polycystic Kidney Disease Gene Causes Polycystic Liver Disease. Kidney360. 2020;1(10):1068–1076. doi:10.34067/kid.0002522020 [PubMed: 33554127]
7. Woollard JR, Punyashtiti R, Richardson S, et al. A mouse model of autosomal recessive polycystic kidney disease with biliary duct and proximal tubule dilatation. Kidney Int. 2007;72(3):328–336. doi:10.1038/sj.ki.5002294 [PubMed: 17519956]
8. Masyuk TV, Masyuk AI, Lorenzo Pisarello M, et al. TGR5 contributes to hepatic cystogenesis in rodents with polycystic liver diseases through cyclic adenosine monophosphate/Gαs signaling. Hepatology. 2017;66(4):1197–1218. doi:10.1002/hep.29284 [PubMed: 28543567]
9. Masyuk T, Masyuk A, Trussoni C, et al. Autophagy-mediated reduction of miR-345 contributes to hepatic cystogenesis in polycystic liver disease. JHEP Rep. 2021;3(5):100345. Published 2021 Aug 5. doi:10.1016/j.jhepr.2021.100345 [PubMed: 34568801]
10. Locatelli L, Cadamuro M, Spirlì C, et al. Macrophage recruitment by fibrocystin-defective biliary epithelial cells promotes portal fibrosis in congenital hepatic fibrosis. Hepatology. 2016;63(3):965–982. doi:10.1002/hep.28382 [PubMed: 26645994]

11. Azzolin L, Panciera T, Soligo S, et al. YAP/TAZ incorporation in the β-catenin destruction complex orchestrates the Wnt response. Cell. 2014;158(1):157–170. doi:10.1016/j.cell.2014.06.013 [PubMed: 24976009]
12. Daulat AM, Borg JP. Wnt/Planar Cell Polarity Signaling: New Opportunities for Cancer Treatment. Trends Cancer. 2017;3(2):113–125. doi:10.1016/j.trecan.2017.01.001 [PubMed: 28718442]
13. Daulat AM, Wagner MS, Walton A, et al. The Tumor Suppressor SCRIB is a Negative Modulator of the Wnt/β-Catenin Signaling Pathway. Proteomics. 2019;19(21–22):e1800487. doi:10.1002/pmic.201800487 [PubMed: 31513346]
14. Piccolo S, Dupont S, Cordenonsi M. The biology of YAP/TAZ: hippo signaling and beyond. Physiol Rev. 2014;94(4):1287–1312. doi:10.1152/physrev.00005.2014 [PubMed: 25287865]
15. Zheng HX, Wu LN, Xiao H, Du Q, Liang JF. Inhibitory effects of dobutamine on human gastric adenocarcinoma. World J Gastroenterol. 2014;20(45):17092–17099. doi:10.3748/wjg.v20.i45.17092 [PubMed: 25493021]
16. Ohgushi M, Minaguchi M, Sasai Y. Rho-Signaling-Directed YAP/TAZ Activity Underlies the Long-Term Survival and Expansion of Human Embryonic Stem Cells. Cell Stem Cell. 2015;17(4):448–461. doi:10.1016/j.stem.2015.07.009 [PubMed: 26321201]
17. Dupont S, Morsut L, Aragona M, et al. Role of YAP/TAZ in mechanotransduction. Nature. 2011;474(7350):179–183. doi:10.1038/nature10137 [PubMed: 21654799]
18. Chen WS, Cao Z, Krishnan C, Panjwani N. Verteporfin without light stimulation inhibits YAP activation in trabecular meshwork cells: Implications for glaucoma treatment. Biochem Biophys Res Commun. 2015;466(2):221–225. doi:10.1016/j.bbrc.2015.09.012 [PubMed: 26361148]
19. Gallagher AR, Esquivel EL, Briere TS, et al. Biliary and pancreatic dysgenesis in mice harboring a mutation in Pkhd1. Am J Pathol. 2008;172(2):417–429. doi:10.2353/ajpath.2008.070381 [PubMed: 18202188]
20. Lodillinsky C, Infante E, Guichard A, et al. p63/MT1-MMP axis is required for in situ to invasive transition in basal-like breast cancer. Oncogene. 2016;35(3):344–357. doi:10.1038/onc.2015.87 [PubMed: 25893299]
21. Cadamuro M, Spagnuolo G, Sambado L, et al. Low-Dose Paclitaxel Reduces S100A4 Nuclear Import to Inhibit Invasion and Hematogenous Metastasis of Cholangiocarcinoma. Cancer Res. 2016;76(16):4775–4784. doi:10.1158/0008-5472.CAN-16-0188 [PubMed: 27328733]
22. Jiang L, Sun L, Edwards G, et al. Increased YAP Activation Is Associated With Hepatic Cyst Epithelial Cell Proliferation in ARPKD/CHF. Gene Expr. 2017;17(4):313–326. doi:10.3727/105221617X15034976037343 [PubMed: 28915934]
23. Wang KC, Yeh YT, Nguyen P, et al. Flow-dependent YAP/TAZ activities regulate endothelial phenotypes and atherosclerosis. Proc Natl Acad Sci U S A. 2016;113(41):11525–11530. doi:10.1073/pnas.1613121113 [PubMed: 27671657]
24. Di Benedetto A, Mottolese M, Sperati F, et al. The Hippo transducers TAZ/YAP and their target CTGF in male breast cancer. Oncotarget. 2016;7(28):43188–43198. doi:10.18632/oncotarget.9668 [PubMed: 27248471]
25. Nagasawa-Masuda A, Terai K. Yap/Taz transcriptional activity is essential for vascular regression via Ctgf expression and actin polymerization. PLoS One. 2017;12(4):e0174633. doi:10.1371/journal.pone.0174633 [PubMed: 28369143]
26. Shome D, von Woedtke T, Riedel K, Masur K. The HIPPO Transducer YAP and Its Targets CTGF and Cyr61 Drive a Paracrine Signalling in Cold Atmospheric Plasma-Mediated Wound Healing. Oxid Med Cell Longev. 2020;2020:4910280. doi:10.1155/2020/4910280 [PubMed: 32104533]
27. Ruffolo RR Jr. The pharmacology of dobutamine. Am J Med Sci. 1987;294(4):244–248. doi:10.1097/00000441-198710000-00005 [PubMed: 3310640]
28. Ito T, Taniguchi H, Fukagai K, Okamuro S, Kobayashi A. Inhibitory mechanism of FAT4 gene expression in response to actin dynamics during Src-induced carcinogenesis. PLoS One. 2015;10(2):e0118336. Published 2015 Feb 13. doi:10.1371/journal.pone.0118336 [PubMed: 25679223]
29. Zanconato F, Cordenonsi M, Piccolo S. YAP/TAZ at the Roots of Cancer. Cancer Cell. 2016;29(6):783–803. doi:10.1016/j.ccell.2016.05.005 [PubMed: 27300434]

30. Feng J, Gou J, Jia J, Yi T, Cui T, Li Z. Verteporfin, a suppressor of YAP-TEAD complex, presents promising antitumor properties on ovarian cancer. Onco Targets Ther. 2016;9:5371–5381. Published 2016 Aug 29. doi:10.2147/OTT.S109979 [PubMed: 27621651]

31. Cohen J, Raviv S, Adir O, Padmanabhan K, Soffer A, Luxenburg C. The Wave complex controls epidermal morphogenesis and proliferation by suppressing Wnt-Sox9 signaling. J Cell Biol. 2019;218(4):1390–1406. doi:10.1083/jcb.201807216 [PubMed: 30867227]

32. Cohen J, Luxenburg C. Wave of the future: involvement of actin polymerization in the regulation of tissue growth and shape. Mol Cell Oncol. 2019;6(5):e1609877. Published 2019 May 29. doi:10.1080/23723556.2019.1609877 [PubMed: 31528690]

33. Xu D, Lv J, He L, et al. Scribble influences cyst formation in autosomal-dominant polycystic kidney disease by regulating Hippo signaling pathway. FASEB J. 2018;32(8):4394–4407. doi:10.1096/fj.201701376RR [PubMed: 29529391]

34. Walter TJ, Vanderpool C, Cast AE, Huppert SS. Intrahepatic bile duct regeneration in mice does not require Hnf6 or Notch signaling through Rbpj. Am J Pathol. 2014;184(5):1479–1488. doi:10.1016/j.ajpath.2014.01.030 [PubMed: 24631193]

35. Masyuk TV, Masyuk AI, LaRusso NF. Therapeutic Targets in Polycystic Liver Disease. Curr Drug Targets. 2017;18(8):950–957. doi:10.2174/1389450116666150427161743 [PubMed: 25915482]

36. Quinn HM, Vogel R, Popp O, et al. YAP and β-Catenin Cooperate to Drive Oncogenesis in Basal Breast Cancer. Cancer Res. 2021;81(8):2116–2127. doi:10.1158/0008-5472.CAN-20-2801 [PubMed: 33574090]

37. Mannaerts I, Leite SB, Verhulst S, et al. The Hippo pathway effector YAP controls mouse hepatic stellate cell activation. J Hepatol. 2015;63(3):679–688. doi:10.1016/j.jhep.2015.04.011 [PubMed: 25908270]

38. Kim I, Fu Y, Hui K, et al. Fibrocystin/polyductin modulates renal tubular formation by regulating polycystin-2 expression and function. J Am Soc Nephrol. 2008;19(3):455–468. doi:10.1681/ASN.2007070770 [PubMed: 18235088]

39. McNeill H Planar cell polarity and the kidney. J Am Soc Nephrol. 2009;20(10):2104–2111. doi:10.1681/ASN.2008111173 [PubMed: 19762494]

40. Skouloudaki K, Puetz M, Simons M, et al. Scribble participates in Hippo signaling and is required for normal zebrafish pronephros development. Proc Natl Acad Sci U S A. 2009;106(21):8579–8584. doi:10.1073/pnas.0811691106 [PubMed: 19439659]

41. Zhang X, Zheng X, Lou Y, et al. β-catenin inhibitors suppress cells proliferation and promote cells apoptosis in PC9 lung cancer stem cells. Int J Clin Exp Pathol. 2017;10(12):11968–11978. [PubMed: 31966561]

42. Nowell CS, Odermatt PD, Azzolin L, et al. Chronic inflammation imposes aberrant cell fate in regenerating epithelia through mechanotransduction. Nat Cell Biol. 2016;18(2):168–180. doi:10.1038/ncb3290 [PubMed: 26689676]

43. Konsavage WM Jr, Kyler SL, Rennoll SA, Jin G, Yochum GS. Wnt/β-catenin signaling regulates Yes-associated protein (YAP) gene expression in colorectal carcinoma cells. J Biol Chem. 2012;287(15):11730–11739. doi:10.1074/jbc.M111.327767 [PubMed: 22337891]

44. Banales JM, Masyuk TV, Gradilone SA, Masyuk AI, Medina JF, LaRusso NF. The cAMP effectors Epac and protein kinase a (PKA) are involved in the hepatic cystogenesis of an animal model of autosomal recessive polycystic kidney disease (ARPKD). Hepatology. 2009;49(1):160–174. doi:10.1002/hep.22636 [PubMed: 19065671]

45. Gradilone SA, Masyuk TV, Huang BQ, et al. Activation of Trpv4 reduces the hyperproliferative phenotype of cystic cholangiocytes from an animal model of ARPKD. Gastroenterology. 2010;139(1):304–14.e2. doi:10.1053/j.gastro.2010.04.010 [PubMed: 20399209]

46. Humbert PO, Grzeschik NA, Brumby AM, Galea R, Elsum I, Richardson HE. Control of tumourigenesis by the Scribble/Dlg/Lgl polarity module. Oncogene. 2008;27(55):6888–6907. doi:10.1038/onc.2008.341 [PubMed: 19029932]

47. Wang Y, Pan P, Wang Z et al. β-catenin-mediated YAP signaling promotes human glioma growth. J Exp Clin Cancer Res. 2017;36(136). doi:10.1186/s13046-017-0606-1

48. Tao J, Calvisi DF, Ranganathan S, et al. Activation of β-catenin and Yap1 in human hepatoblastoma and induction of hepatocarcinogenesis in mice. Gastroenterology. 2014;147(3):690–701. doi:10.1053/j.gastro.2014.05.004 [PubMed: 24837480]

49. Pinto C, Giordano DM, Maroni L, Marzioni M. Role of inflammation and proinflammatory cytokines in cholangiocyte pathophysiology. Biochim Biophys Acta Mol Basis Dis. 2018;1864(4 Pt B):1270–1278. doi:10.1016/j.bbadis.2017.07.024 [PubMed: 28754451]

50. Cadamuro M, Girardi N, Gores GJ, Strazzabosco M, Fabris L. The Emerging Role of Macrophages in Chronic Cholangiopathies Featuring Biliary Fibrosis: An Attractive Therapeutic Target for Orphan Diseases. Front Med (Lausanne). 2020;7:115. Published 2020 Apr 21. doi:10.3389/fmed.2020.00115 [PubMed: 32373615]

51. Yonem O, Bayraktar Y. Clinical characteristics of Caroli's disease. World J Gastroenterol. 2007;13(13):1930–1933. doi:10.3748/wjg.v13.i13.1930 [PubMed: 17461492]

52. Dey A, Varelas X, Guan KL. Targeting the Hippo pathway in cancer, fibrosis, wound healing and regenerative medicine. Nat Rev Drug Discov. 2020;19(7):480–494. doi:10.1038/s41573-020-0070-z [PubMed: 32555376]

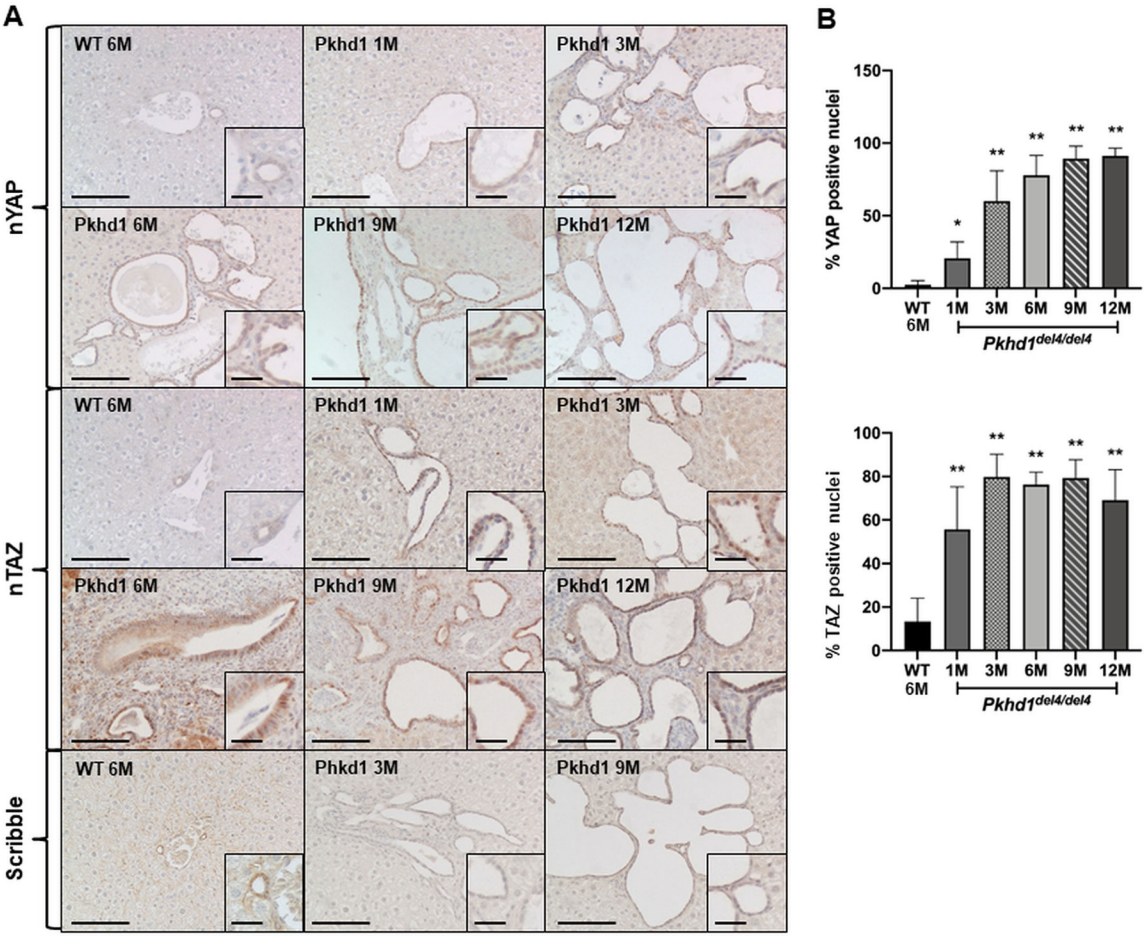

Figure 1. In *Pkhd1*$^{del4/del4}$ mice expression of nYAP and nTAZ in biliary cysts increases over time on the contrary to Scribble.

(A) Representative micrographs of WT mice at 6 months and *Pkhd1*$^{del4/del4}$ mice at different ages showing nuclear expression of YAP (nYAP) and TAZ (nTAZ), and of Scribble; nYAP and nTAZ were increased in biliary cysts of *Pkhd1*$^{del4/del4}$ mice through all the different ages (1, 3, 6, 9, and 12 months). On the other hand, Scribble was expressed at cell-cell junctions in WT, whereas its expression was nearly absent in mutated mice at all ages. (B) Computer-assisted morphometric analysis of nYAP and nTAZ showed increased expression of both proteins in biliary cysts in *Pkhd1*$^{del4/del4}$ at 1, 3, 6, 9, and 12 months vs WT. Scale bar: 100μm, insets: 25μm; *p<0.05 vs WT, and **p<0.01 vs WT using two-tail *t* test, n=4 each.

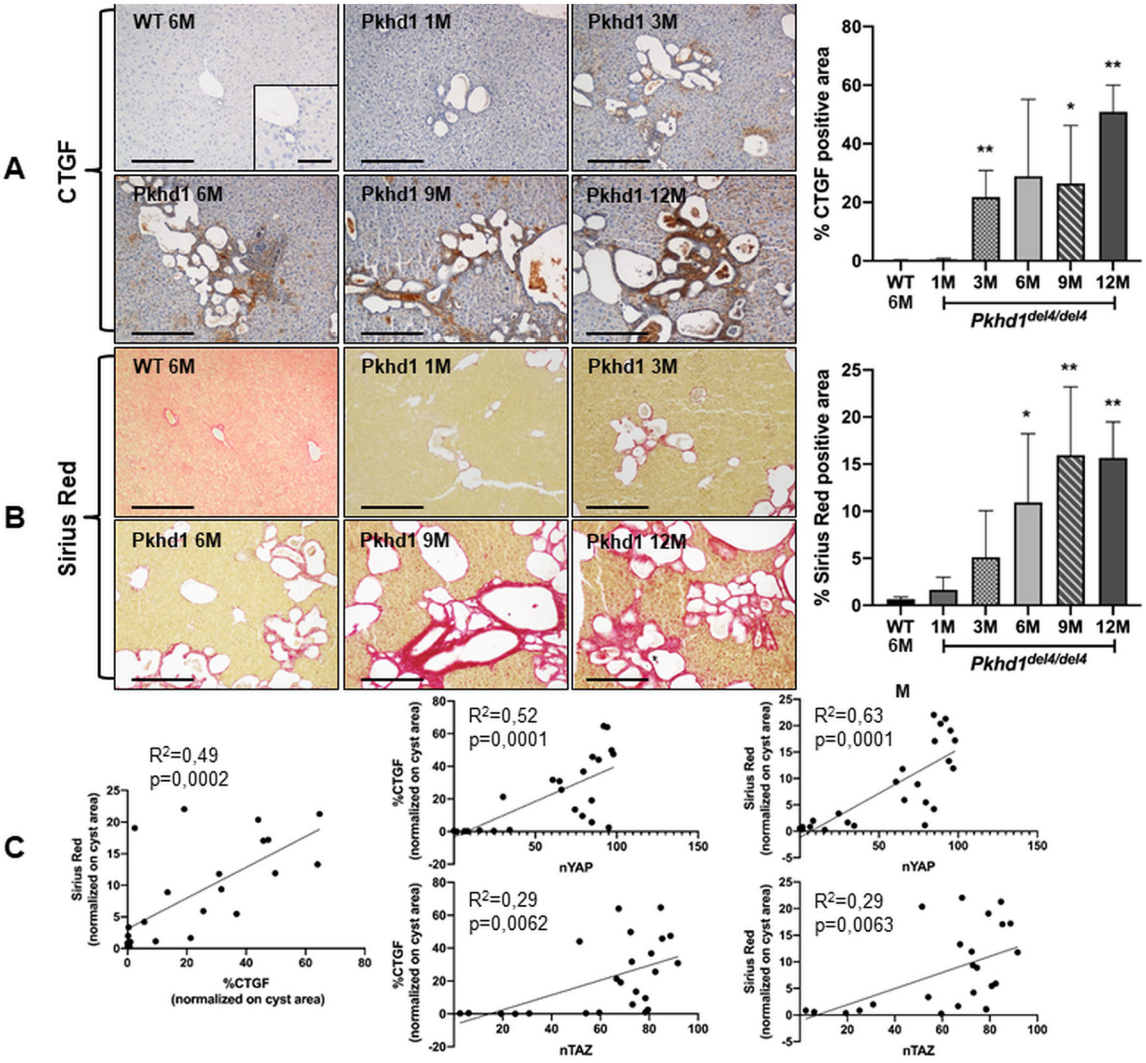

Figure 2. In *Pkhd1*$^{del4/del4}$ mice, CTGF and Sirius Red expression increases over the time of the disease and correlates with both nYAP and nTAZ immunoreactivity.

Representative micrographs showing CTGF expression (A) and fibrosis distribution (Sirius Red staining) (B) in WT at 6 month and *Pkhd1*$^{del4/del4}$ mice at different ages (1, 3, 6, 9, and 12 months). By computer-assisted morphological analysis, expression of CTGF (A) and extent of fibrosis (B) increased in a time-dependent fashion in slides of *Pkhd1*$^{del4/del4}$ mice starting from 3 and 6 months, respectively. (C) Extent of CTGF and Sirius Red correlated one with each other, and with both nYAP and nTAZ expression. Scale bar: 200μm, inset: 50μm; *p<0.05 vs WT, and **p<0.01 vs WT using two-tail *t* test, n=4 each. Correlation was calculated by Pearson's test.

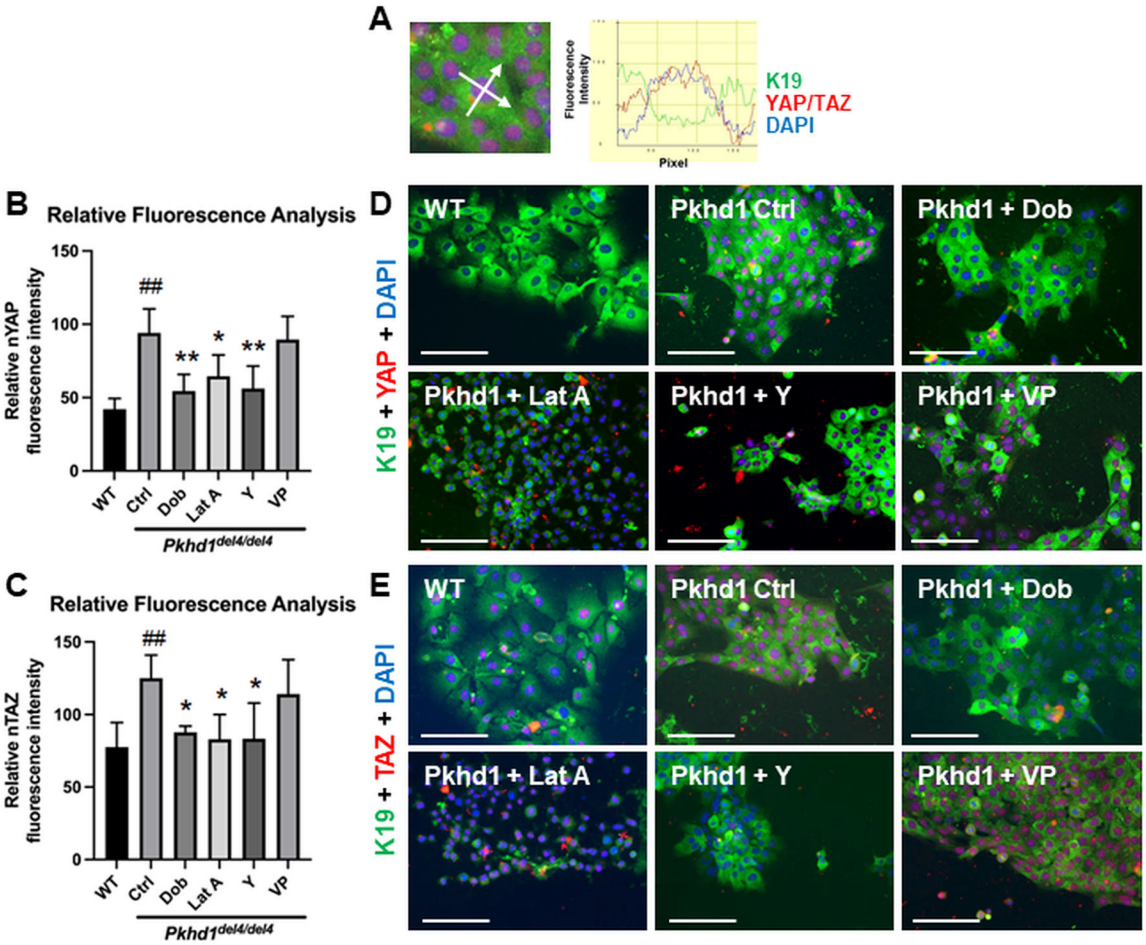

Figure 3. Cholangiocytes from *Pkhd1*$^{del4/del4}$ mice harbor nYAP and nTAZ expression, an effect reduced by treatments with different chemical inhibitors.

(A) Representative images used for the relative fluorescence analysis. Following immunofluorescence for YAP/TAZ (red) and K19 (green, biliary marker), two orthogonal lines, centered on the nucleus, were traced, to generate a plot measuring the relative intensity of the tree channels (red = YAP, green = K19, blue = DAPI). For each traced line, the highest peak of intensity for the red channel intersecting the blue area was calculated. (B, C) In *Pkhd1*$^{del4/del4}$ cholangiocytes, constitutive expression of nYAP and nTAZ was abrogated by treatment with Dob, Lat A and Y, but not with VP; in WT cholangiocytes, nYAP and nTAZ were noticeably reduced compared with mutated cells. (D, E) Representative images showing the effects of the different inhibitors on YAP/TAZ nuclear expression (red), assessed by relative fluorescence intensity analysis. Scale bar: 100μm; $^{\#\#}$p<0.01 vs WT, *p<0.05 vs *Pkhd1*$^{del4/del}$ ctrl, and **p<0.01 vs *Pkhd1*$^{del4/del}$ ctrl using one-way ANOVA test, n=4.

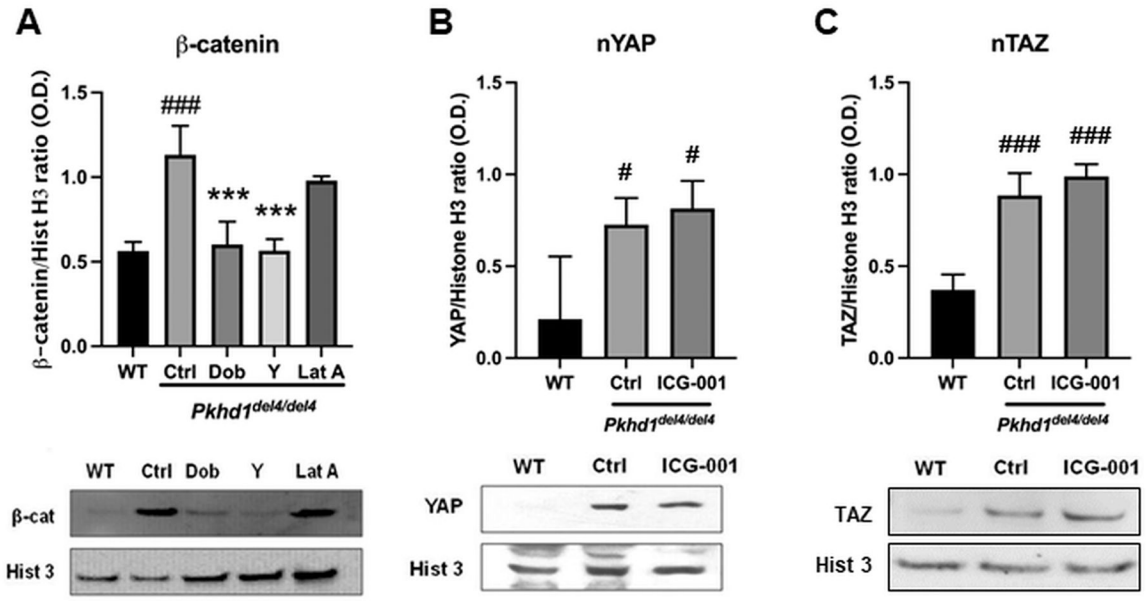

Figure 4. Chemical inhibition of YAP/TAZ modulates β-catenin nuclear expression, in *Pkhd1*$^{del4/del4}$ cholangiocytes.

Protein expression of YAP, TAZ and β-catenin were assessed by Western blot in nuclear cell fractions. (A) Nuclear expression of β-catenin was significantly higher in *Pkhd1*$^{del4/del4}$ compared with WT cholangiocytes. Treatment with Dob and Y significantly reduced the nuclear expression of β-catenin in *Pkhd1*$^{del4/del4}$ cells, indicating a YAP-dependence of β-catenin expression. Conversely, in *Pkhd1*$^{del4/del4}$ cholangiocytes, nuclear expression of both YAP (B) and TAZ (C) were not abrogated by β-catenin suppression with ICG-001. $^{\#}p<0.05$ vs WT, $^{\#\#}p<0.01$ vs WT, $^{\#\#\#}p<0.001$ vs WT, ***$p<0.001$ vs *Pkhd1*$^{del4/del}$ ctrl using one-way ANOVA test, n=3 to 4.

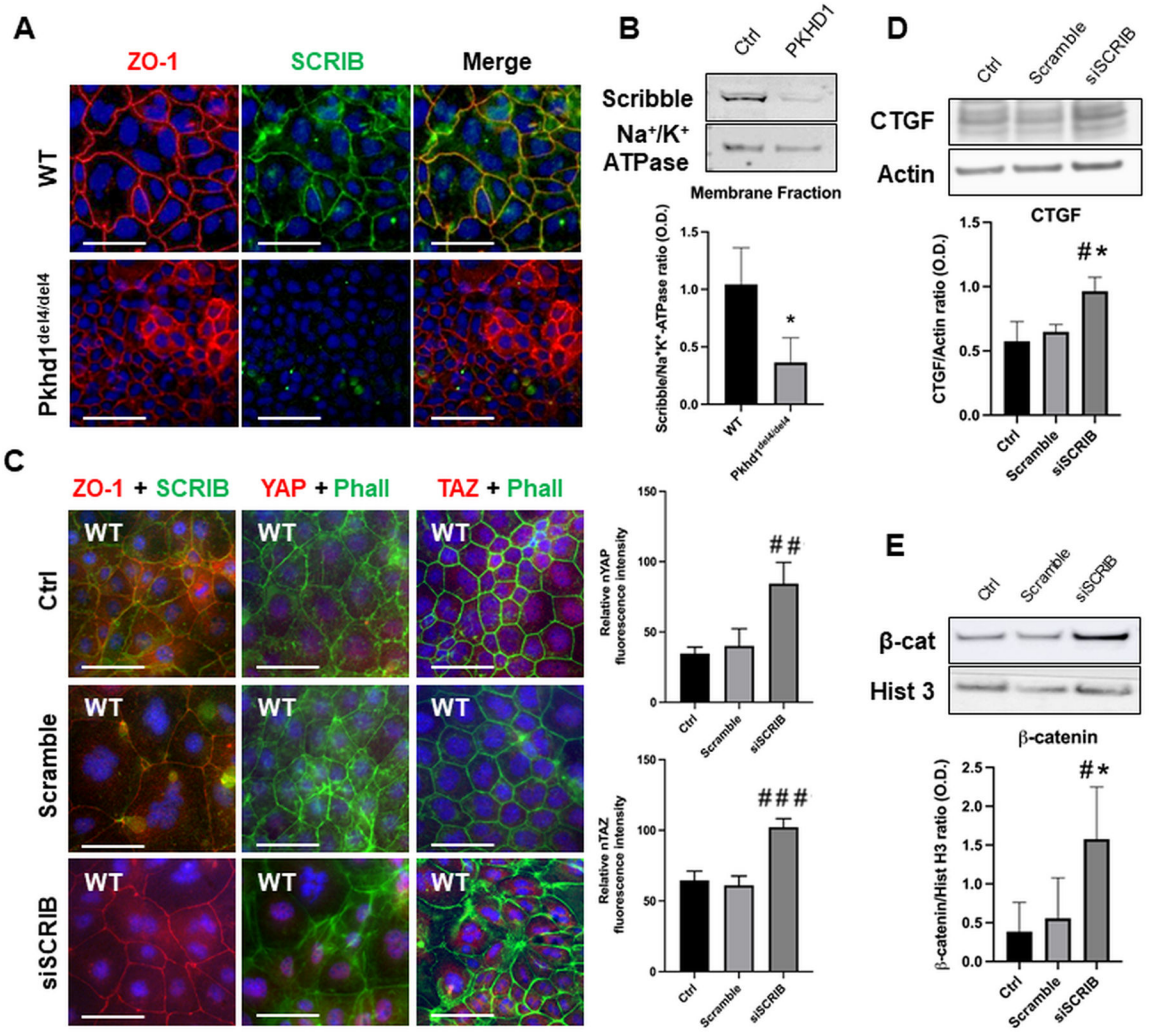

Figure 5. In *Pkhd1*$^{del4/del4}$ cholangiocytes, Scribble expression at the membrane is reduced compared with WT cells, and in WT cells, its inhibition by siRNA induces YAP and TAZ nuclearization.

(A) In WT cholangiocytes, Scribble (green) showed the proper expression at the cell junctions, as demonstrated by its co-localization (yellow) with ZO-1 (red, tight junction marker), in contrast with *Pkhd1*$^{del4/del4}$ cholangiocytes that lacked Scribble. (B) These data were also confirmed by WB analysis of membrane fraction from WT and *Pkhd1*$^{del4/del4}$ cells. Na^+/K^+ ATPase served as normalizing protein for membranes. (C) WT biliary cells with siRNA-mediated silencing of Scribble, showed YAP and TAZ (red) accumulation in the nucleus in conjunction with loss of Scribble membrane expression as showed by IF staining and by plots of relative fluorescence analysis for nYAP and nTAZ (n=3 each). Phalloidin (green) was used to highlight the morphology of the cytoskeleton. (D) CTGF expression, a known downstream effector of YAP, was up-regulated following genetic inhibition of Scribble (siSCRIB), as respect to untreated controls (Ctrl) and Scramble, consistent with a constitutive inhibitory tone exerted by Scribble on YAP signaling (n=3). (E) Notably, in WT cells, siSCRIB treatment induced nuclear accumulation of β-catenin, showing a dependence of its nuclear shuttling with the presence at membrane of Scribble (n=5). Scale bar: 50μm;

$^{\#}p<0.05$ vs ctrl, $p^{\#\#}<0.01$ vs ctrl and $^{\#\#\#}p<0.001$ vs ctrl, and *$p<0.05$ WT or vs scramble using one-way ANOVA test.

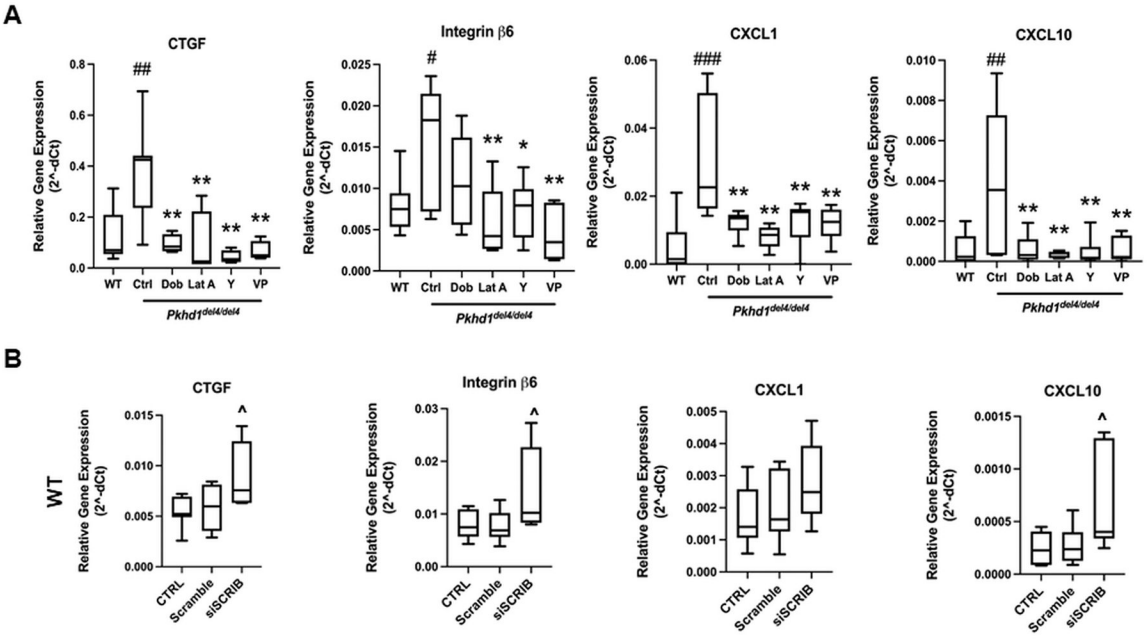

Figure 6. Chemical and genetic manipulation of the YAP/Scribble pathway modulates the expression of pro-inflammatory mediators in *Pkhd1*$^{del4/del4}$ and WT cholangiocytes.

(A) YAP inhibition abolished the constitutive increased expression of CTGF, β6 integrin, CXCL1 and CXCL10 of *Pkhd1*$^{del4/del4}$ compared with WT cholangiocytes. (B) On the other hand, genetic silencing of Scribble in WT cholangiocytes induced the up-regulation of CTGF, β6 and CXCL10. $^{\#}$p<0.05 vs WT, $^{\#\#}$p<0.01 vs WT, $^{\#\#\#}$p<0.001 vs WT, *p<0.05 vs *Pkhd1*$^{del4/del}$ ctrl, **p<0.01 vs *Pkhd1*$^{del4/del}$ ctrl, ^p<0.05 vs ctrls using one-way ANOVA test, n=4 to 7.

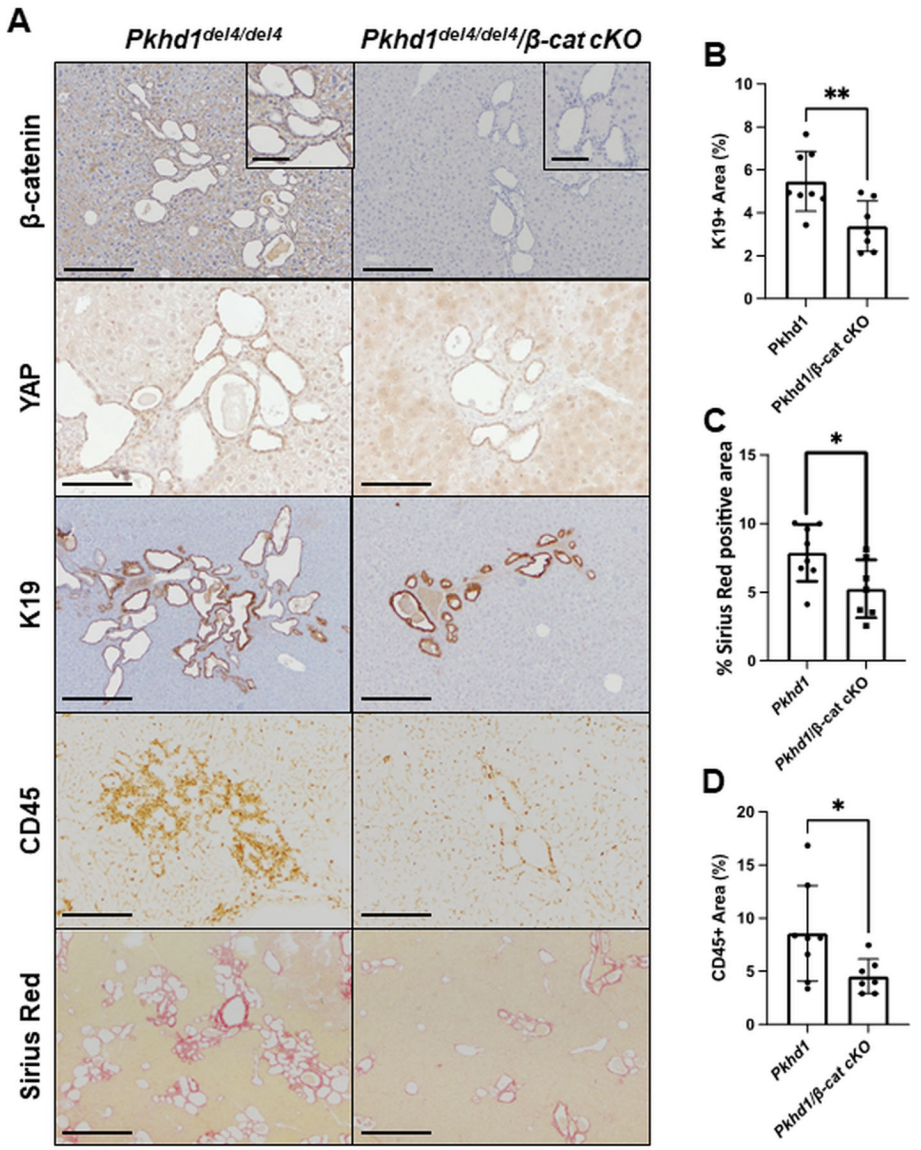

Figure 7. In *Pkhd1*$^{del4/del4}$/*β-cat cKO* mice, cyst size, inflammatory infiltrate and fibrosis deposition are reduced as respect to *Pkhd1*$^{del4/del4}$ controls.

(A) Representative micrographs of *Pkhd1*$^{del4/del4}$ and *Pkhd1*$^{del4/del4}$/*β-cat cKO* mice confirming the absence of β-catenin expression in *Pkhd1*$^{del4/del4}$/*β-cat cKO* mice and accumulation of nYAP in both mouse models. *Pkhd1*$^{del4/del4}$/*β-cat cKO* showed a significant reduction in the extent of K19 (cholangiocytes), CD45 (inflammatory infiltrate), and Sirius Red (fibrosis deposition) as compared to *Pkhd1*$^{del4/del4}$ mice. (B-D) These data were confirmed by computer-assisted morphometric analysis. Scale bar: 200μm, insets: 50μm; *p<0.05 vs *Pkhd1*$^{del4/del4}$, **p<0.01 vs *Pkhd1*$^{del4/del4}$ using two-tail *t* test.

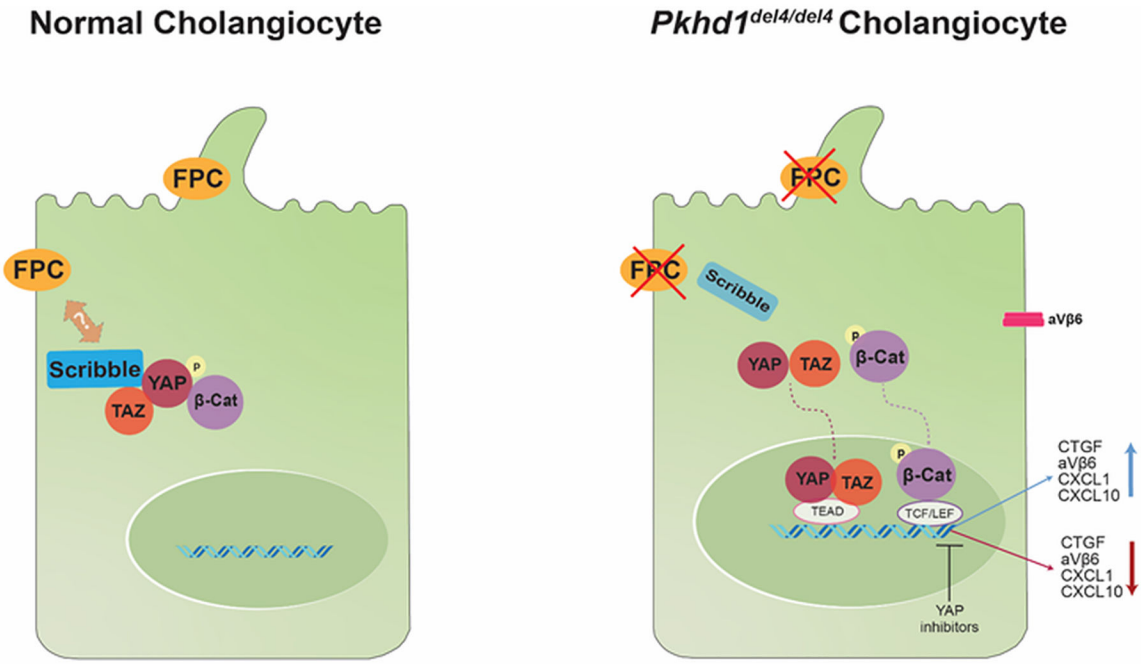

Figure 8. Working model illustrating the pathogenetic mechanism dependent on the interplay between Scribble/YAP/β-catenin in conditions of FPC deficiency.

In normal cholangiocytes, Scribble retains YAP into the cytoplasm in a phosphorylated and inactive state. YAP, as a part of the β-catenin destruction complex, binds β-catenin, impeding its release and consequent nuclear translocation. In CHF, defects in FPC interfere with Scribble/YAP interaction, with consequent YAP dephosphorylation that leads, on the one side, to the nuclear migration of YAP and on the other, to the release of β-catenin from the destruction complex, enabling it to enter the nucleus together with YAP. Once in the nucleus, YAP and β-catenin activate their own transcriptional programs, which govern the typical fibroinflammatory reaction displayed by FPC-defective cholangiocytes. Chemokines and growth factors (CXCL1, CXCL10 and CTGF) are richly secreted and integrin αVβ6, the local activator of TGF-β, is strongly up-regulated, with recruitment of macrophages and activation of myofibroblasts.